A&A 368, 824–834 (2001)
DOI: 10.1051/0004-6361:20010091

Astronomy & Astrophysics

Global molecular gas properties of Seyfert galaxies⋆

I. The observational data

S. J. Curran[1,2], A. G. Polatidis[1], S. Aalto[1], and R. S. Booth[1]

[1] Onsala Space Observatory, Chalmers University of Technology, 439 92 Onsala, Sweden
[2] European Southern Observatory, Casilla 19001, Santiago 19, Chile

Received 19 December 2000 / Accepted 12 January 2001

Abstract. In this paper we present large-scale maps of the $J = 1 \rightarrow 0$ transitions of CO and HCN in a sample of 7 near-by Seyfert galaxies. These are the first large-scale maps of CO in NGCs 2273 and 5033 and of HCN in all of the sample. From the maps we tabulate the integrated intensities at various extents and calculate the corresponding luminosities. The CO luminosities are compared with those of Young et al. (1995). It is our intention to use these results in conjunction with those of a distant Seyfert sample, in Paper II (Curran et al. 2001a), in order to analyse the differences in molecular gas luminosities and distributions, not only between the full sample and other galaxy types, but between the near-by and distant samples. Immediately, from the observational data we see that the HCN is distributed beyond the central beam (∼1 kpc) in much of the sample. We consider this to be an important result which we will discuss further in Paper II.

Key words. galaxies: Seyfert–galaxies: abundances–galaxies: ISM

1. Introduction

From a survey of the $J = 1 \rightarrow 0$ transitions of CO and HCN in the central positions of 20 Seyfert galaxies, we (Curran et al. 2000)[1] found a HCN/CO luminosity ratio of ≈1/6 for the "distant" sample in which the telescope beam-width exceeds ≈10 kpc (galaxies with a recessional velocity of $v \gtrsim 4000$ km s^{-1}), i.e. a global ratio similar to that of ultra-luminous infrared galaxies (ULIRGs) and over 10 times the ratio for normal spiral galaxies. This relatively high abundance of HCN, which traces dense molecular gas, in comparison to the bulk component of the gas, as traced by the CO, suggests a significant presence of molecular hydrogen densities in excess of $\gtrsim 10^4$ cm^{-3} in the Seyfert sample. The relative luminosities of CO, HCN and the far infrared (FIR) radiation lead to the conclusion $\frac{L_{\rm FIR}}{L_{\rm CO}}$ (distant Seyferts) $\gtrsim 10 \frac{L_{\rm FIR}}{L_{\rm CO}}$ (normal spirals), from which the excess far infrared flux may arise from an active galactic nucleus in addition to the star-burst activity. Furthermore, some questions were raised about the differences in the molecular gas luminosities and distributions between the distant and the near-by[2] samples (see Paper II). In order to resolve this issue, in this work we present maps of the near-by sources, NGCs 1068, 1365, 2273, 5033 and 6814[3] (in conjunction with the two other near-by Seyferts, visible from SEST[4]; the Circinus galaxy and NGC 4945), and give the global luminosity values obtained from these, the results of which will be discussed in the forthcoming Paper II.

2. Observations

The Southern sources in the sample were observed in several sessions between December 1998 and November 2000 with the 15 m SEST at La Silla, Chile. For HCN $1 \rightarrow 0$ and CO $1 \rightarrow 0$ we used the 100 GHz (SESIS) and 115 GHz (IRAM) receivers, respectively. Since the 115 GHz can be

Send offprint requests to: S. J. Curran,
e-mail: sjc@oso.chalmers.se

⋆ Based on results collected at the European Southern Observatory, La Silla, Chile and Onsala Space Observatory, Sweden.

[1] These galaxies were chosen on the grounds that they provide a good sample of Seyferts. As well as this, they constitute the same sample of Heckman et al. (1989), thus enabling us to also test their finding that type 2 Seyferts have higher molecular gas abundances than type 1s (see Curran 2000b and Paper II).

[2] Galaxies where $v \lesssim 4000$ km s^{-1}.

[3] Note that since we failed to detect HCN in NGCs 5347 and 7172 (Curran et al. 2000), we will not include these sources in this work.

[4] The Swedish-ESO Sub-millimetre Telescope is operated jointly by ESO and the Swedish National Facility for Radio Astronomy, Onsala Space Observatory, Chalmers University of Technology.

Table 1. Beam sizes and efficiencies

Transition	ν [GHz]	HPBW [″]		$\eta_{\rm mb}$	
		OSO	SEST	OSO	SEST
HCN $1 \rightarrow 0$	89	44	57	0.59	0.75
CO $1 \rightarrow 0$	115	33	45	0.50	0.70
CO $2 \rightarrow 1$	230	–	22	–	0.50

used simultaneously with the 230 GHz receiver, we also mapped the CO $2 \rightarrow 1$ transition. All receivers were tuned to single-sideband mode and typical system temperatures, on the $T_{\rm A}^*$-scale, were 200 K at 89 GHz, 200 to 300 K at 115 GHz and 300 K at 230 GHz. The backends were acousto-optical spectrometers with 1440 channels and a channel width of 0.7 MHz. We used dual-beam switching with a throw of about 12′ in azimuth, and pointing errors were typically 3″ rms on each axis. The intensity was calibrated using the chopper-wheel method. For all of the observing runs the weather was excellent, and only the removal of linear baselines was required.

The Northern sources in the sample were observed over one continuous 7 day session in September 2000 with the 20 m telescope at Onsala Space Observatory (OSO). Both the CO $1 \rightarrow 0$ and HCN $1 \rightarrow 0$ transitions were observed with the SIS 100 GHz receiver. The backend was a filterbank with a bandwidth of 512 MHz and a channel separation of 1 MHz. We used a similar dual-beam switching as the SEST observations and obtained similar pointing errors. The weather was good (typical system temperatures were around 250 to 400 K at 89 GHz and 450 to 600 K at 115 GHz) and, as with the SEST data, only linear baselines were removed. The beam sizes and efficiences for the two telescopes at various transitions are given in Table 1.

3. Results

The observational results are summarised in Table 2 and the maps are shown in Figs. 1 to 6, where the intensity scale is $T_{\rm A}^*$ and velocities are shown relative to local standard of rest. Note that although the SEST maps are shown at their observed spacings, the global integrated intensities (Table 2), like the OSO observations, are calculated for a map spacing of one beam (as in Table 1).

In Table 3 the luminosities are summmarised. These are calculated by multiplying the average integrated intensity by the area of the map (e.g. as in Sandqvist et al. 1995). Since there may be some ambiguity due to how much area is actually mapped[5], we constrain the value by multiplying the global integrated intensity at single beam spacing over the estimated source size[6], which gives a similar result as calculated by the average integrated intensity over the mapped area. In Table 3 the values given are:

1. The luminosity over the central beam[7], i.e. as in Table 3 of Curran et al. (2000);
2. Over the full CO mapped region;
3. Over the HCN[8] mapped region.

The last two values allow us to state the CO/HCN luminosity ratios, not only over the central beam, but also over the whole (molecular gas region) of the galaxy as well as over the region of the HCN emission. We discuss our results for each source below and compare them with previously published CO observations. We are not aware of any large-scale HCN maps of these galaxies.

3.1. NGC 1068

Our value of the global CO luminosity (Table 3) is comparable with that Planesas et al. (1989) who get, also from single dish observations, $L_{\rm CO\ 1\rightarrow0} = 3.8\ 10^3$ K km s^{-1} kpc^2 over a partial map spanning $120'' \times 120''$ (cf. Fig. 1). Both results are consistent with those of Young et al. (1995), see Sect. 4.

Concerning HCN, note that the central integrated intensity is similar to that obtained previously at Onsala (11 ± 1 K km s^{-1}, Curran et al. 2000), although, due to the larger SEST beam, the central luminosity is slightly higher (cf. $0.09 \pm 0.01\ 10^3$ K km s^{-1} kpc^2).

3.2. NGC 1365

Our CO values agree well with those previously published by Sandqvist et al. (1995); $1.7\ 10^3$ K km s^{-1} kpc^2 over the central beam and $5.3\ 10^3$ K km s^{-1} kpc^2 at 20″ spacing over $204'' \times 164''$.

Again the central HCN result agrees well with our previous measurement of $0.16 \pm 0.031\ 10^3$ K km s^{-1} kpc^2 (Curran et al. 2000).

3.3. NGC 2273

We are not aware of any large-scale maps of either CO or HCN in this galaxy. The central CO value agrees well with that of $0.041 \pm 0.003\ 10^3$ K km s^{-1} kpc^2 (Curran et al. 2000).

[5] For example, although HCN $1 \rightarrow 0$ is mapped to $68'' \times 68''$ in NGC 1365 (Fig. 2), the HPBW of 57″ increases this to $\lesssim 125'' \times 125''$ due to the beam extending beyond the "mapped region".

[6] Obtained by assuming that the source distribution on the sky is Gaussian and deconvolving the telescope response (HBPW) from the full-width half-maximum (FWHM) diameter, e.g. Dahlem et al. (1993). The source sizes are tabulated and discussed in Paper II.

[7] In the angular size of the corresponding transition, Table 1.

[8] From now on, unless otherwise stated, HCN or CO refers to the $1 \rightarrow 0$ transition for the appropriate molecule.

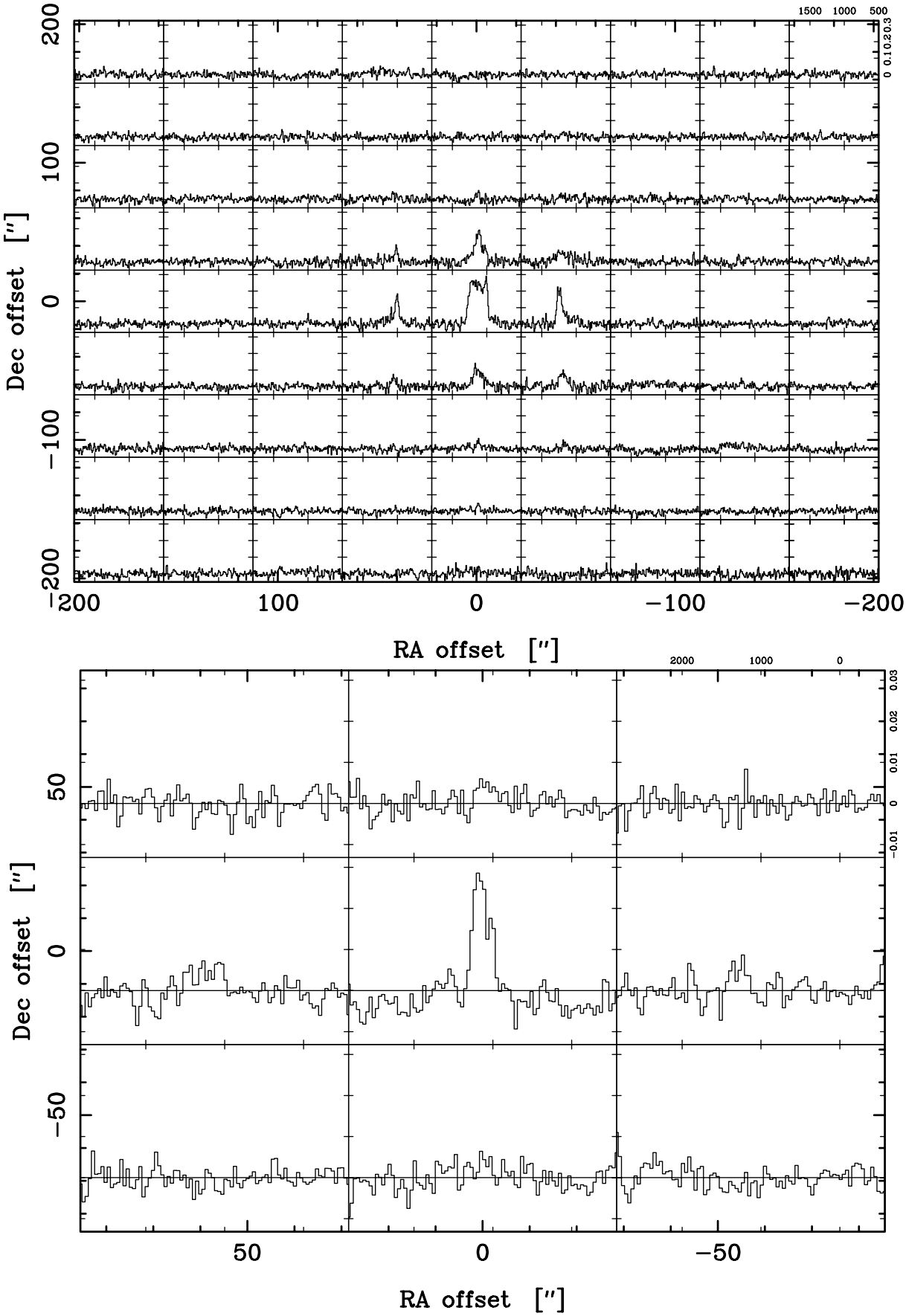

Fig. 1. Top: CO $1 \rightarrow 0$ in NGC 1068 over the full mapped region. The spacing is $44''$ and the velocity resolution is 10 km s^{-1}. Bottom: HCN $1 \rightarrow 0$ in NGC 1068 over the full mapped region. The spacing is $57''$ and the velocity resolution is 40 km s^{-1}

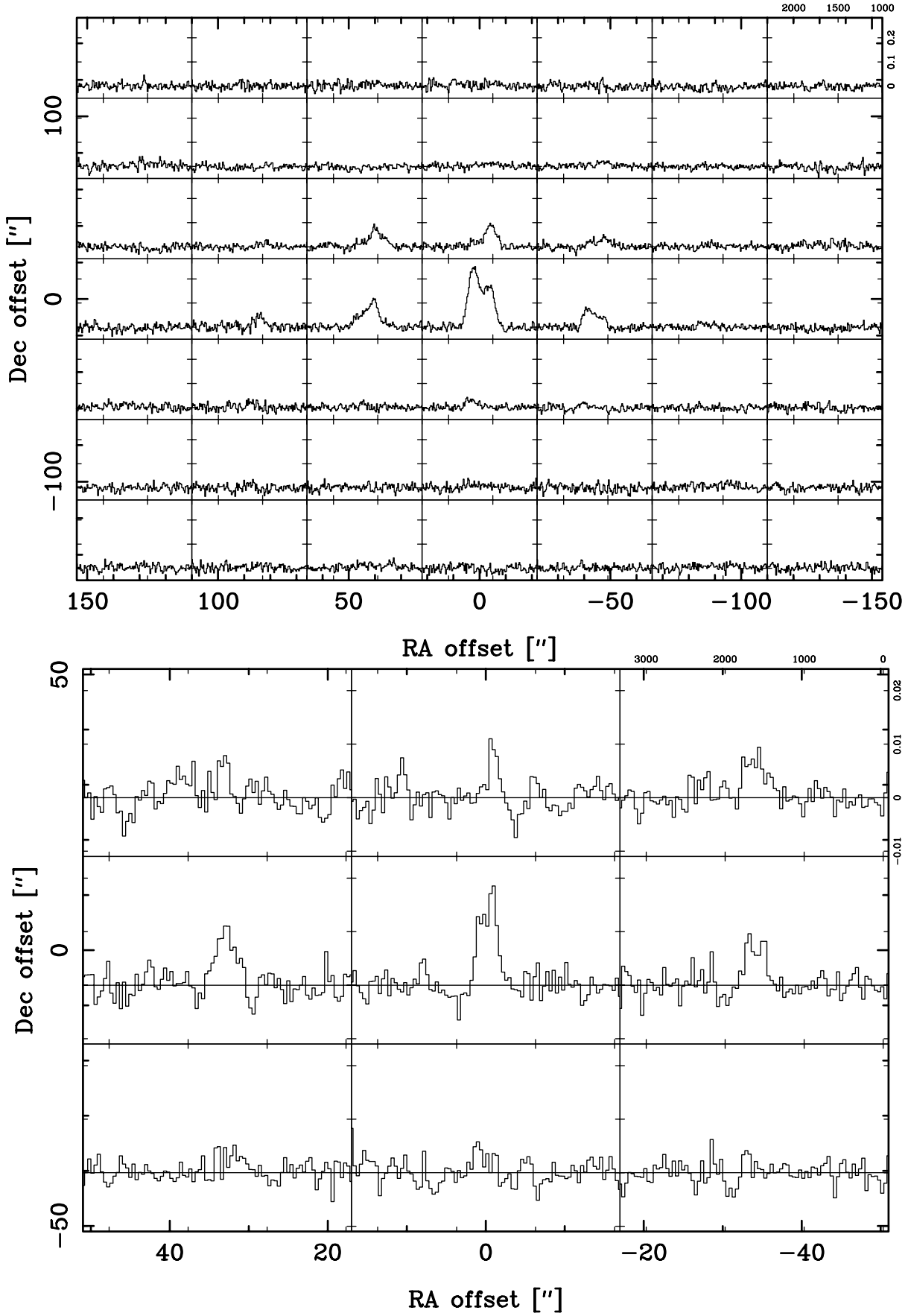

Fig. 2. Top: CO $1 \rightarrow 0$ in NGC 1365 over the full mapped region. The spacing is $44''$ and the velocity resolution is 10 km s^{-1}. Bottom: HCN $1 \rightarrow 0$ in NGC 1365 over $68'' \times 68''$ of the $136'' \times 136''$ region mapped. The spacing is $34''$ and the velocity resolution is 40 km s^{-1}

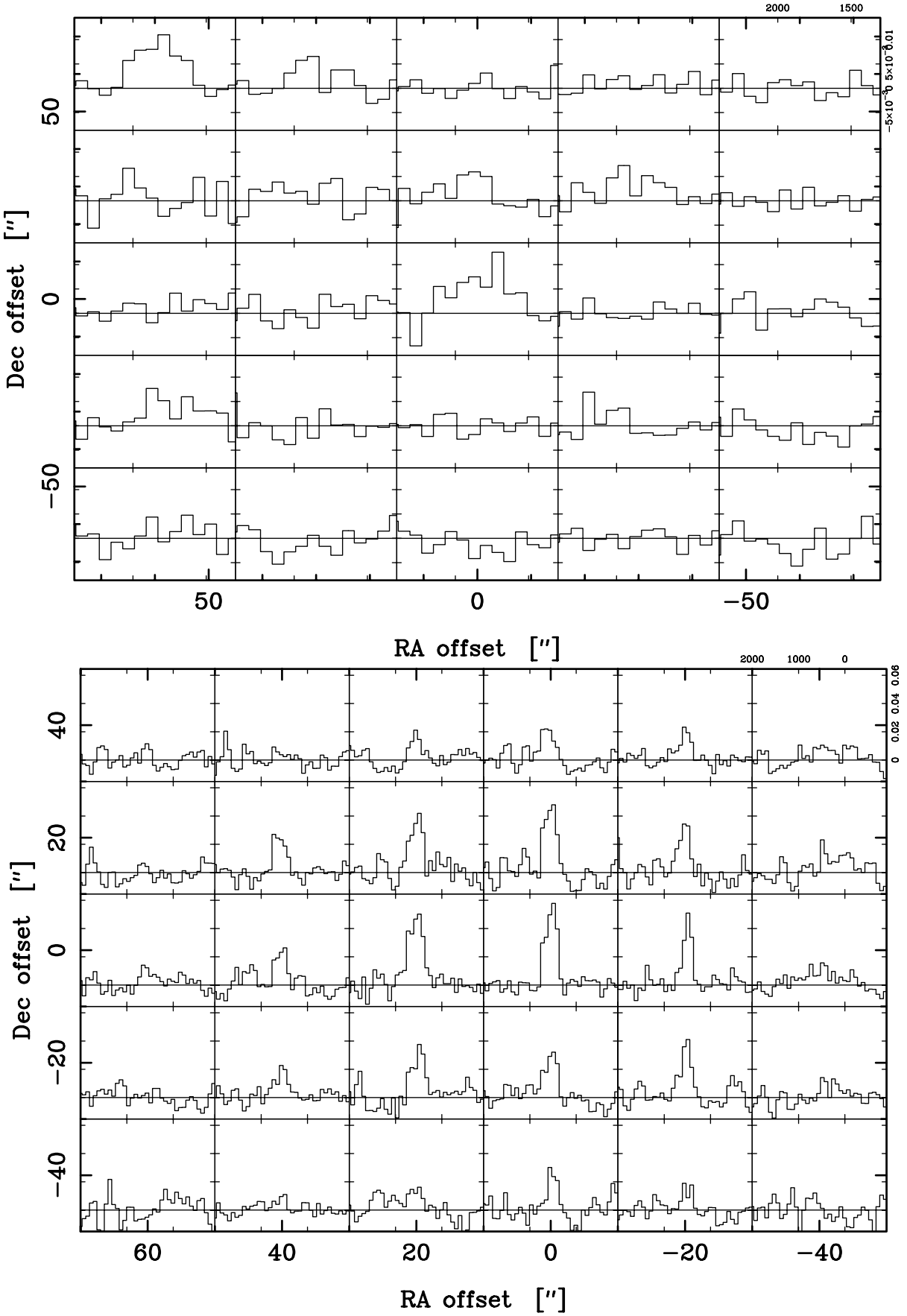

Fig. 3. Top: CO $1 \rightarrow 0$ in NGC 2273 over the full mapped region. The spacing is $30''$ and the velocity resolution is 80 km s^{-1}. There were no HCN detections in this galaxy. Bottom: HCN $1 \rightarrow 0$ in NGC 4945 over $100'' \times 80''$ of the $140'' \times 120''$ mapped region. The spacing is $20''$ and the velocity resolution is 80 km s^{-1}

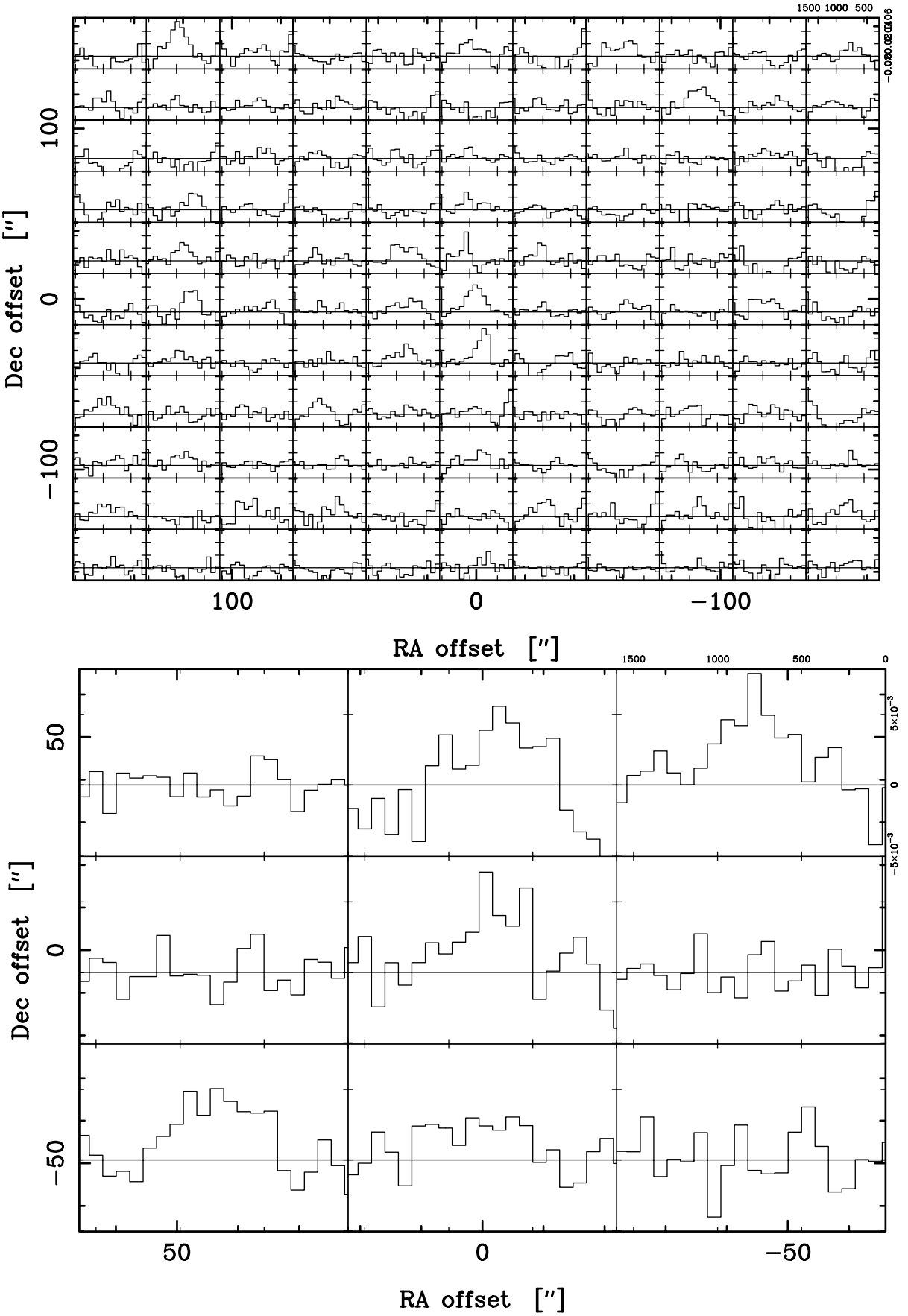

Fig. 4. Top: CO $1 \rightarrow 0$ in NGC 5033 over the full mapped region. The spacing is $30''$ and the velocity resolution is 80 km s^{-1}. Bottom: HCN $1 \rightarrow 0$ in NGC 5033 over the full mapped region. The spacing is $44''$ and the velocity resolution is 80 km s^{-1}. The emission at $(-44'', 44'')$ could correspond to that in position $(-30'', 30'')$ of the CO map

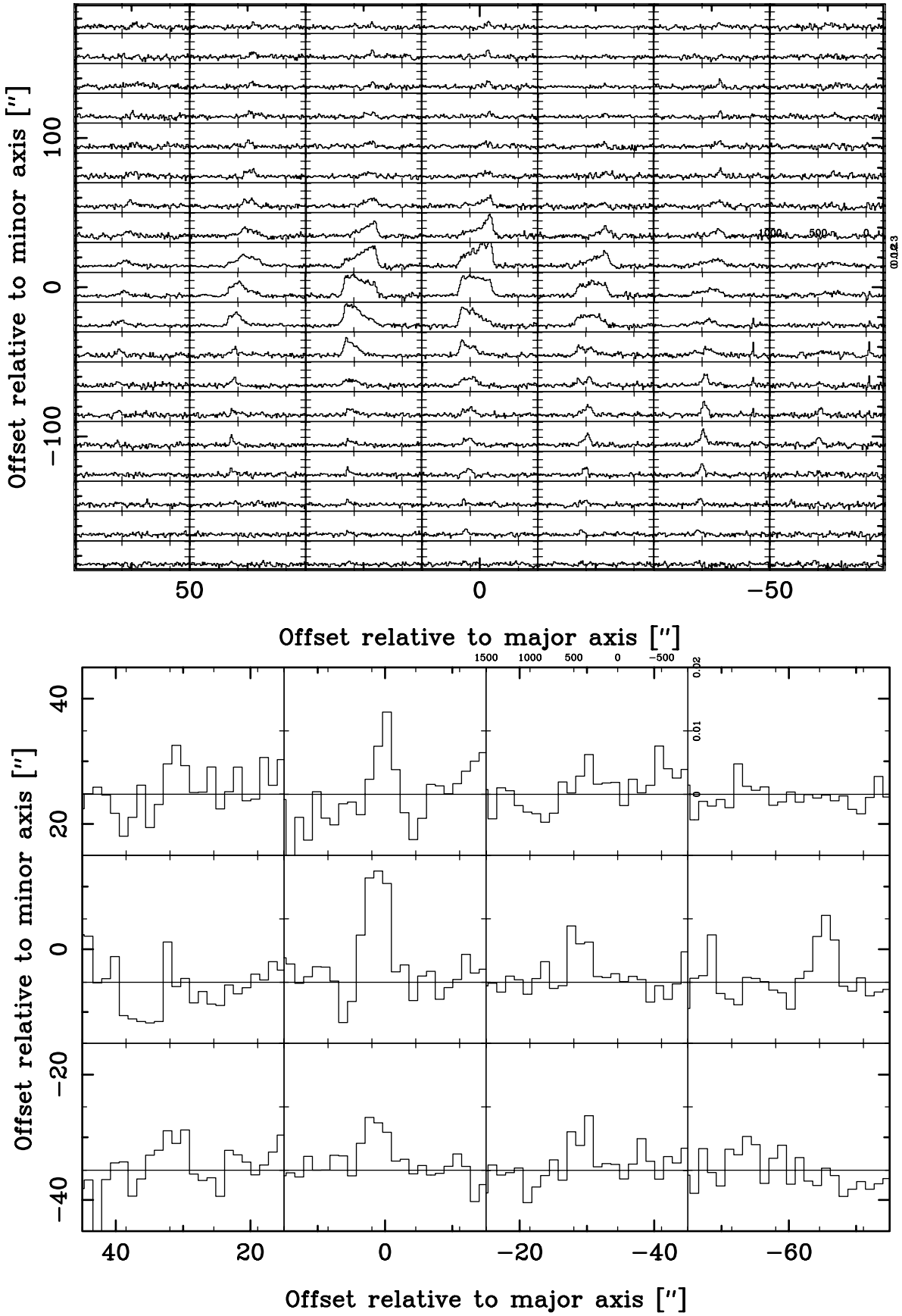

Fig. 5. Top: CO $1 \rightarrow 0$ in Circinus over $120'' \times 360''$ of the $120'' \times 500''$ mapped region. The antenna temperature increment is 0.1 K, the spacing is $20''$ and the velocity increment, of 10 km s^{-1} resolution, is 500 km s^{-1}. Bottom: HCN $1 \rightarrow 0$ in Circinus over the full mapped region. The spacing is $30''$ and the velocity resolution is 100 km s^{-1}

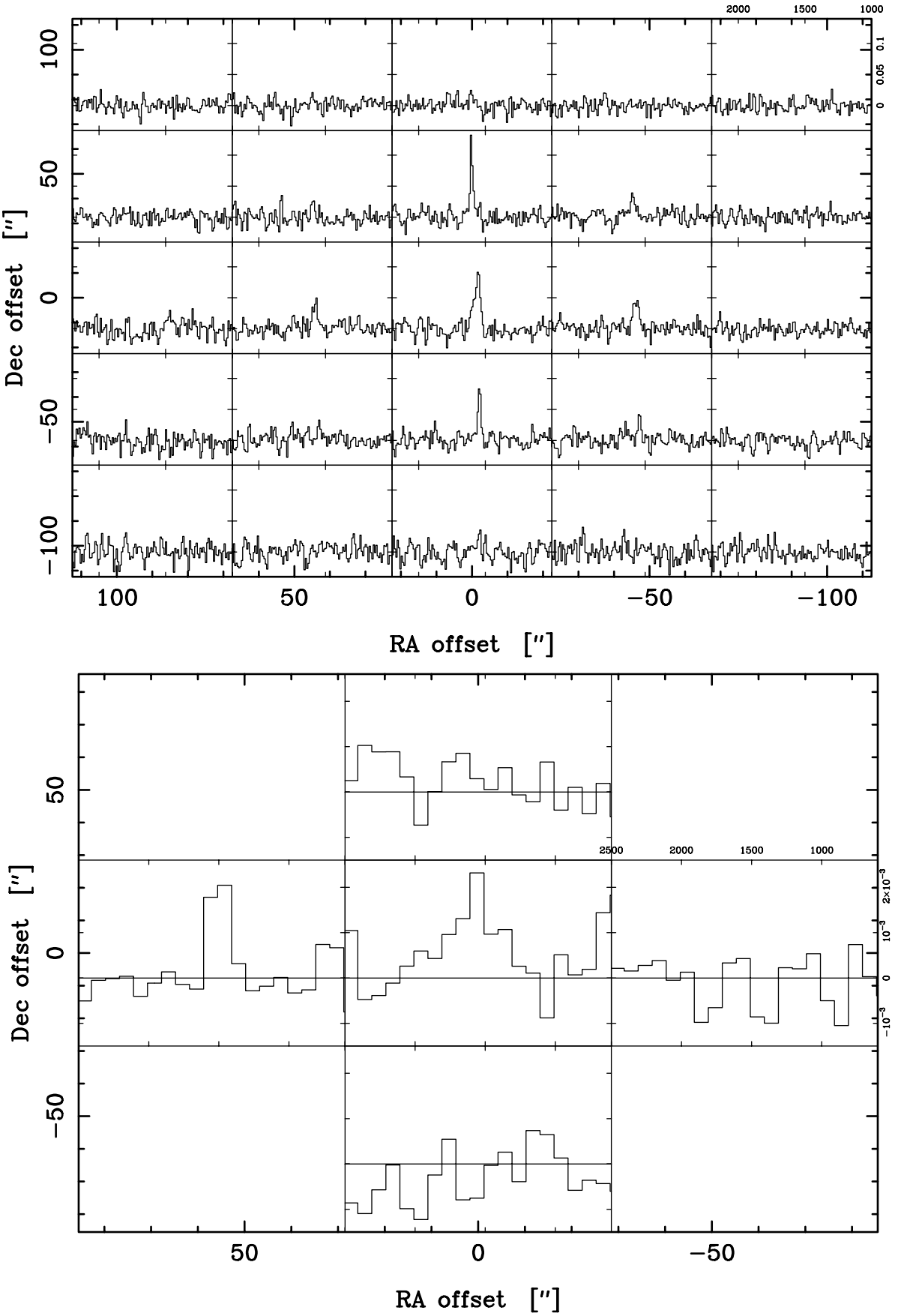

Fig. 6. Top: CO $1 \rightarrow 0$ in NGC 6814 over the full mapped region. The spacing is $44''$ and the velocity resolution is 10 km s^{-1}. Bottom: HCN $1 \rightarrow 0$ in NGC 6814 over the full mapped region. The spacing is $57''$ and the velocity resolution is 100 km s^{-1}

Table 2. The 5 galaxies of Curran et al. (2000) with $v < 4000$ km s^{-1} in which HCN was detected. NGC 4945 and Circinus have been added in order to increase the sample (see Curran et al. 2001b). In the table "Teles." refers to the telescope used with the observed date given. The final three main columns refer to the main-beam brightness temperatures, $I_{\rm mb}$ (centre) and $\int I_{\rm mb}$ (global) [K km s^{-1}], measured for the corresponding transition, where the results have been rounded to two figures (because of $\eta_{\rm mb}$) and the errors and upper limits are according to 1σ (defined by the noise). Concerning the larger uncertainties: In NGC 1365 these arise from differences over the 4 day observing run due to the uncertainty in the focusing of the telescope over this period (April 2000). The resulting values compare well with those previously (Curran et al. 2000). For NGC 4945 the CO $1 \rightarrow 0$ results are from the data of Dahlem et al. (1993) and the CO $2 \rightarrow 1$ data from our own December 1998 observations: The uncertainties are obtained by comparing the central spectra with those of Curran et al. (2001b), after taking into account the slightly different main beam efficiences between the 1988 and post 1993 epochs. In Circinus the same focusing uncertainties responsible in the case of NGC 1365 during the CO observations, caused a reduction in antenna temperature (cf. Curran et al. 1998), thus giving the larger uncertainties. *In NGC 6814 since our map quality is so poor (Fig. 6), this value is taken from Fig. 3 of Curran et al. (2000). We also used our original detection to determine the moment/baseline boxes over the map, giving the values quoted as well as a central value of 0.60 ± 0.15 K km s^{-1}

Galaxy	Teles.	Date(s)	HCN $1 \rightarrow 0$		CO $1 \rightarrow 0$		CO $2 \rightarrow 1$	
			Centre	Global	Centre	Global	Centre	Global
NGC 1068	SEST	9/00 & 11/00	10 ± 1	13 ± 2	107 ± 3	360 ± 10	133 ± 1	320 ± 10
NGC 1365	SEST	4/00	5.5 ± 0.5	13 ± 1	100 ± 10	300 ± 30	150 ± 10	> 300
NGC 2273	OSO	9/00	0.5 ± 0.3	< 0.7	4 ± 1	≈ 4	–	–
NGC 4945	SEST	12/98 & 6/00	23 ± 1	41 ± 2	510 ± 30	3400 ± 700	740 ± 40	3700 ± 500
NGC 5033	OSO	9/00	2.2 ± 0.7	8 ± 2	30 ± 3	200 ± 60	–	–
Circinus	SEST	6/99, 4/00 & 6–7/00	7 ± 1	24 ± 5	150 ± 30	550 ± 100	190 ± 30	2100 ± 300
NGC 6814	SEST	8/00	$0.45 \pm 0.08^*$	1.1 ± 0.3	6.4 ± 0.6	31 ± 3	4.4 ± 0.6	18 ± 3

Table 3. The luminosities of the near-by sample over the beam, HCN extent of emission and mapped region [$\times 10^3$ K km s^{-1} kpc^2]. Here and in Table 5, D refers to the distance to the galaxy [Mpc] (assuming a Hubble parameter of $H_0 = 75$ km s^{-1} Mpc^{-1}) and $L_{\rm FIR}$ [10^{10} $L_\odot$] is the far infrared luminosity computed using the FIR flux (Lonsdale et al. 1985, Heckman et al. 1989). Note that the CO in NGC 1068 was observed at SEST as opposed to OSO (Curran et al. 2000) and so the larger beam gives a correspondingly larger value of $L_{\rm CO\ 1\rightarrow0}$ over the central beam

Galaxy	D	$L_{\rm HCN\ 1\rightarrow0}$		$L_{\rm CO\ 1\rightarrow0}$			$L_{\rm CO\ 2\rightarrow1}$		$L_{\rm FIR}$
		Beam	Map	Beam	HCN Map	Map	Beam	Map	
NGC 1068	15	0.12 ± 0.03		0.91	≈ 1.1	2.4	0.28	1.62 ± 0.07	7.4
NGC 1365	20	0.13 ± 0.01	≈ 0.25	1.4 ± 0.1	≈ 2.7	≈ 4.7	0.54 ± 0.07	≈ 5.0	6.8
NGC 2273	25	≈ 0.01	< 0.07	0.05 ± 0.01	≈ 0.06	≈ 0.08	–	–	0.66
NGC 4945	4	≈ 0.02	0.04 ± 0.01	0.25 ± 0.01	≈ 0.8	≈ 1.4	0.09 ± 0.01	≈ 0.6	0.91
NGC 5033	12	0.011 ± 0.003	0.022 ± 0.005	0.08 ± 0.01	≈ 0.3	0.6 ± 0.1	–	–	0.53
Circinus	4	0.006 ± 0.002		0.09 ± 0.02	≈ 0.20	≈ 0.27	0.03	≈ 0.35	0.62
NGC 6814	21	0.011 ± 0.002	0.035 ± 0.006	0.10 ± 0.01	≈ 0.42		0.017 ± 0.002	0.19 ± 0.03	0.66
Average	14	0.04	0.08	0.4	0.8	1.4	0.2	1.6	2.5

3.4. NGC 4945

We adopt a distance of 3.7 Mpc (Mauersberger et al. 1996) (although distance estimates to NGC 4945 vary somewhat, e.g. 6.7 Mpc according to Dahlem et al. 1993, Forbes & Norris 1998). The choice of value has no effect on the relative luminosities (i.e. ratios). Note that while the central CO $1 \rightarrow 0$ integrated intensity compares well with that obtained by Mauersberger et al. (1996) ($\approx$450 K km s^{-1}), the global value from *this* data is around 3 times greater than actually published by Dahlem et al.(1993) (900 ± 50 K km s^{-1}), Table 2.

The central HCN integrated intensity compares well with that of Curran et al. (2001b) (24 ± 2 K km s^{-1}).

3.5. NGC 5033

Again we are not aware of any large-scale maps, although both the CO and HCN luminosities agree with those previously determined, i.e. 0.093 ± 0.006 and 0.014 ± 0.002 10^3 K km s^{-1} kpc^2, respectively (Curran et al. 2000).

Note that due to the relatively close proximity and vastness of this galaxy, we may be far from having global CO values and that the "structure" in our map may be due to some structure within the galaxy, e.g. spiral arms (Thean et al. 1997 and references therein).

3.6. Circinus

The new values agree well with those from the maps of 1988 and 1993 (see Curran et al. 1998), i.e.

$\approx$0.3 10^3 K km s^{-1} kpc^2 for both the CO 1 $\rightarrow$ 0 and 2 $\rightarrow$ 1 transitions.

Concerning the HCN, the central integrated intensity agrees (within uncertainties) with that of Curran et al. (2001b), i.e. 5.2 ± 0.8 K km s^{-1}. Note that (blue-shifted) HCN may also be detected at $-60''$ along the minor axis, which corresponds to the (approaching) NW molecular outflow (Curran et al. 1999) and where a tentative detection of HCO^+ has been made (see Curran 2000a).

3.7. NGC 6814

With no large-scale maps available, again the CO luminosity agrees with that previously obtained, i.e. 0.118 ± 0.002 10^3 K km s^{-1} kpc^2, although due to the weak emission (a central integrated intensity of $\approx$0.5 K km s^{-1}, Curran et al. 2000), no HCN was detected over the time allocated to map this molecule[9].

4. Erratum: Comparison of the results with those of Young et al. (1995)

At this point we should note an error in Table 3 of Curran et al. (2000): When calculating the global CO luminosity values using the global fluxes of Young et al. (1995), we multiplied these over the whole flux region, when in actual fact these should be multiplied over the source size (where the flux falls to 50%). Unfortunately this is not available in Young et al. (1995) but the diameter within which 70% of the flux is contained is given, allowing us to assign upper limits to their results. These are compared with our results in Table 4.

Table 4. The global CO 1 $\rightarrow$ 0 luminosities [$\times 10^3$ K km s^{-1} kpc^2] compared with those of Young et al. (1995) (Young)

NGC	1068	2273	5033	6814	7469
Our	2.4	$\approx$0.08	0.6 ± 0.01	$\approx$0.42	2.00 ± 0.09
Young	< 4	< 0.04	< 1.7	< 0.45	1.9 ± 0.3

Note that for NGC 1068 the Young et al. (1995) observation is over a diameter of $84''$ and hence captures most of the flux (Fig. 1). This can be seen in their value of 120 ± 40 K km s^{-1}, cf. ours of 133 K km s^{-1} for the global integrated intensity.

NGC 2273 is only observed over a diameter of $30''$, although it appears that most of the flux is sampled, 3.8 ± 0.7 K km s^{-1}, cf. our value of $\approx$4 K km s^{-1} for the global integrated intensity.

NGC 5033 is observed over a diameter of $96''$ and our map (Fig. 4) suggests that there may be emission beyond this.

NGC 6814 is over a diameter of $78''$ which is a similar region to where we find emission (Fig. 6).

[9] The detection of Curran et al. (2000) was new.

For completeness, our previous value for NGC 7469 (Curran et al. 2000), was correct as the source is distant (v = 4900 km s^{-1}) and so the flux contained within the central beam (diameter 10 kpc) determines the global luminosity. Thus with the exception of NGC 2273, the remaining results are at least consistent with those of Young et al. (1995).

5. Summary

We see that our results are mostly in agreement with those previously published (where these exist) and by using the full map (global) values of these in conjunction with those of the distant sample (Curran et al. 2000, Table 5)[10], in Paper II we will analyse these results and draw our conclusions.

Table 5. Recap of the luminosities (with 1σ errors) [$\times 10^3$ K km s^{-1} kpc^2] for the distant sample galaxies in which HCN was detected (adapted from Curran et al. 2000)

Galaxy	D	$L_{\rm CO\ 1\rightarrow0}$	$L_{\rm HCN\ 1\rightarrow0}$	Ratio	$L_{\rm FIR}$
NGC 0034	79	2.3 ± 0.1	0.56 ± 0.07	4.1	14.3
NGC 1667	61	1.18 ± 0.08	0.45 ± 0.06	2.6	4.2
Mrk 231	170	6.0 ± 0.6	1.0 ± 0.2	6.0	128
Mrk 273	150	2.4 ± 0.4	2.4 ± 0.8	$\approx$1	73
NGC 5135	55	2.0 ± 0.1	0.11 ± 0.01	18	9.0
Arp 220	71	2.6 ± 0.1	0.4 ± 0.2	6.5	84
NGC 7130	65	2.6 ± 0.2	0.16 ± 0.02	16	11.9
NGC 7469	65	2.00 ± 0.09	0.25 ± 0.07	8.0	18.2
Average	90	2.6	0.67	6 ± 2	43

Acknowledgements. We wish to thank the referee R. Antonucci for his prompt and helpful comments. Also, Lars E. B. Johansson for his advice, Francisco Azagra at SEST for staying up to monitor the impromtu SEST observations of NGC 1068, Aage Sandqvist for his NGC 1365 data as well as Felipe Mac-Auliffe and Saul Vidal at La Silla for getting the Dahlem et al. (1993) data from 9-track tape, and Susanne Hüttemeister for her permission to use it. This research made use of the NASA/IPAC Extragalactic Database (NED) which is operated by the Jet Propulsion Laboratory, California Institute of Technology, under contract with the National Aeronautics and Space Administration.

References

Curran, S. J., Aalto, S., & Booth, R. S. 2000, A&AS, 141, 193
Curran, S. J., Johansson, L. E. B., Rydbeck, G., & Booth, R. S. 1998, A&A, 338, 863

[10] Where all of the molecular gas is expected to be contained within the central beam (Sect. 1). For example, Young et al. (1995) obtain the same value of $L_{\rm CO\ 1\rightarrow0}$ in an area which is twice the diameter of our beam (at OSO), thus confirming this (see previous section).

Curran, S. J., Rydbeck, G., Johansson, L. E. B., & Booth, R. S. 1999, A&A, 344, 767
Curran, S. J., Aalto, S., Polatidis, A. G., & Booth, R. S. 2001a, A&A, in preparation (Paper II)
Curran, S. J., Johansson, L. E. B., Bergman, P., Heikkilä, A., & Aalto, S. 2001b, A&A, In press
Curran, S. J. 2000a, Ph.D. Thesis, Chalmers University of Technology
Curran, S. J. 2000b, A&AS, 144, 271
Dahlem, M., Golla, G., Whiteoak, J. B., et al. 1993, A&A, 270, 29
Forbes, D. A., & Norris, R. P. 1998, MNRAS, 300, 757
Heckman, T. M., Blitz, L., Wilson, A. S., Armus, L., & Miley, G. K. 1989, ApJ, 342, 735
Lonsdale, C. J., Helou, G., Good, J. C., & Rice, W. 1985, Cataloged Galaxies and Quasars Observed in the IRAS Survey, Jet Propulsion Laboratory, Pasadena
Mauersberger, R., Henkel, C., Whiteoak, J. B., Chin, Y. N., & Tieftrunk, A. R. 1996, A&A, 309, 705
Planesas, P., Gomez-Gonzalez, J., & Martin-Pintado, J. 1989, A&A, 216, 1
Sandqvist, A., Jörsäter, S., & Lindblad, P. 1995, A&A, 295, 585
Thean, A. H. C., Mundell, C. G., Pedlar, A., & Nicholson, R. A. 1997, MNRAS, 290, 15
Young, J. S., Xie, S., Tacconi, L., et al. 1995, ApJS, 98, 219